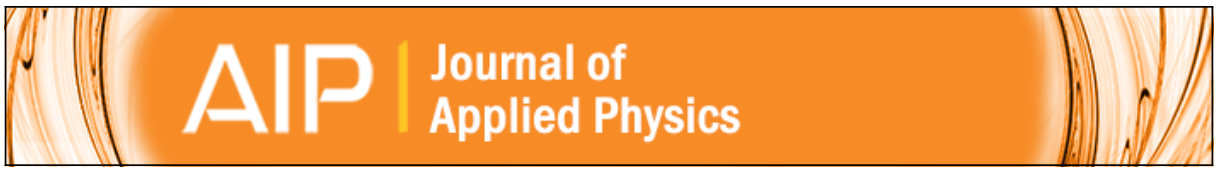

Large infrared absorptance of bimaterial microcantilevers based on silicon high contrast grating

Beomjin Kwon, Myunghoon Seong, Jui-Nung Liu, Matthew R. Rosenberger, Matthew V. Schulmerich, Rohit Bhargava, Brian T. Cunningham, and William P. King

Citation: Journal of Applied Physics **114**, 153511 (2013); doi: 10.1063/1.4825313
View online: http://dx.doi.org/10.1063/1.4825313
View Table of Contents: http://scitation.aip.org/content/aip/journal/jap/114/15?ver=pdfcov
Published by the AIP Publishing

[This article is copyrighted as indicated in the article. Reuse of AIP content is subject to the terms at: http://scitation.aip.org/termsconditions. Downloaded to] IP: 192.17.144.31 On: Fri, 10 Jan 2014 08:09:37

Large infrared absorptance of bimaterial microcantilevers based on silicon high contrast grating

Beomjin Kwon,[1] Myunghoon Seong,[1] Jui-Nung Liu,[2] Matthew R. Rosenberger,[1] Matthew V. Schulmerich,[3,4,5] Rohit Bhargava,[1,2,3,4,5,6] Brian T. Cunningham,[2,3,4] and William P. King[1,2,4,5,a)]

[1]*Department of Mechanical Science and Engineering, University of Illinois Urbana-Champaign, Urbana, Illinois 61801, USA*
[2]*Department of Electrical and Computer Engineering, University of Illinois Urbana-Champaign, Urbana, Illinois 61801, USA*
[3]*Department of Bioengineering, University of Illinois Urbana-Champaign, Urbana, Illinois 61801, USA*
[4]*Micro and Nanotechnology Laboratory, University of Illinois Urbana-Champaign, Urbana, Illinois 61801, USA*
[5]*Beckman Institute for Advanced Science and Technology, University of Illinois Urbana-Champaign, Urbana, Illinois 61801, USA*
[6]*University of Illinois Cancer Center, University of Illinois Urbana-Champaign, Urbana, Illinois 61801, USA*

(Received 5 July 2013; accepted 1 October 2013; published online 17 October 2013)

Manufacturing sensors for the mid-IR spectral region (3–11 μm) are especially challenging given the large spectral bandwidth, lack of convenient material properties, and need for sensitivity due to weak sources. Here, we present bimaterial microcantilevers based on silicon high contrast grating (HCG) as alternatives. The grating integrated into the cantilevers leverages the high refractive index contrast between the silicon and its surrounding medium, air. The cantilevers with HCG exhibit larger active spectral range and absorptance in mid-IR as compared to cantilevers without HCG. We design and fabricate two types of HCG bimaterial cantilevers such that the HCG resonance modes occur in mid-IR spectral region. Based on the measurements using a Fourier transform infrared (FTIR) microspectrometer, we show that the HCG cantilevers have 3–4X wider total IR absorptance bandwidths and 30% larger absorptance peak amplitude than the cantilever without HCG, over the 3–11 μm wavelength region. Based on the enhanced IR absorptance, HCG cantilevers show 13–47X greater responsivity than the cantilever without HCG. Finally, we demonstrate that the enhanced IR sensitivity of the HCG cantilever enables transmission IR spectroscopy with a Michelson interferometer. The HCG cantilever shows comparable signal to noise ratio to a low-end commercial FTIR system and exhibits a linear response to incident IR power. © *2013 AIP Publishing LLC*. [http://dx.doi.org/10.1063/1.4825313]

I. INTRODUCTION

Bimaterial cantilever infrared (IR) detectors are based on the photothermal cantilever bending where the IR light absorption induces temperature rise and the thermal expansion mismatch bending of the cantilever.[1–10] The bimaterial cantilevers have shown a potential as a novel uncooled IR detector by exhibiting IR sensitivity similar to traditional methods but with lower cost and faster response time (~0.1–1 ms).[1,11,12] Published research has shown that a bimaterial cantilever can detect radiative power of 250 pW/Hz$^{0.5}$ at the wavelength of 650 nm,[6] or 1.3 nW/Hz$^{0.5}$ at the wavelength of 10 μm.[3] Focal plane array of bimaterial cantilevers has noise equivalent temperature difference (NETD) of 50–200 mK, which is comparable to the NETD of the most recent microbolometer IR detectors, 35–200 mK.[1,13,14] Thus, multiple groups have explored the applications of bimaterial cantilevers in portable IR imaging[7,9,15,16] and IR spectroscopic systems.[8,17,18]

To make bimaterial cantilever IR detectors practical for applications, despite this progress, it is still necessary to improve their sensitivity.[1,8] Optical and thermomechanical properties determine the cantilever sensitivity, which are related to the cantilever material and geometry.[3,8,17] To improve the cantilever thermomechanical properties, various groups have designed cantilevers with large length, small width, and optimum layer thicknesses to achieve large thermal expansion mismatch stress, small thermal conductance, and small mechanical stiffness.[3,9,19] It was also reported that with an effective thermal isolation to environment, a bimaterial cantilever could measure very small amount of heat flow (>4 pW) and temperature variation (>6.4 μK).[20] However, there have been few efforts to improve the cantilever optical properties.[10] The most common material combination for bimaterial cantilever IR detectors has been silicon nitride and aluminum.[2,3,6,9,10] The cantilevers fabricated with these materials have relatively small optical absorptance over large portion of the mid-IR spectral region due to small imaginary part of refractive index (~0.001–0.01) of silicon nitride.[21] Small optical absorptance has been one of the limiting factors for cantilever sensitivity.

a)Author to whom correspondence should be addressed. Electronic mail: wpk@illinois.edu

 © 2013 AIP Publishing LLC

[This article is copyrighted as indicated in the article. Reuse of AIP content is subject to the terms at: http://scitation.aip.org/termsconditions. Downloaded to] IP: 192.17.144.31 On: Fri, 10 Jan 2014 08:09:37

High-contrast grating (HCG) is periodic grating made of material with higher refractive index than surrounding medium[22] and has recently impacted the device concept of semiconductor optoelectronics and nanophotonics due to its extraordinary features.[22–24] HCG can exhibit broadband high reflection or resonance reflection with high quality factor,[22] which is not commonly obtainable from traditional gratings. HCG can also possess resonance absorption by having a metal layer on its bottom which inverts the reflection spectrum of HCG.[25] Thus, the integration of HCG into an optical system can enhance its absorptance at the spectral region of interest. Here, we report a new type of bimaterial cantilever based on silicon HCG with metallic (aluminum) coating on the bottom for the use across a wide range of mid-IR wavelengths (3–11 μm). By incorporating HCG with the bimaterial cantilever, we aim to enhance cantilever IR absorptance as well as the IR sensitivity of the cantilever. We also demonstrate the application of HCG cantilever into the transmission IR spectroscopy employing a Michelson interferometer as an IR source.

II. CANTILEVER DESIGN AND FABRICATION

We designed and fabricated cantilevers with HCG as described below. Figure 1 shows scanning electron microscope (SEM) images of a fabricated cantilever and the cantilever design. The cantilever has a single crystal silicon layer that consists of a periodic 1D surface corrugation grating structure on top of a waveguide layer. The cantilever has an aluminum coating on the bottom surface. We use lightly doped silicon (nominal doping density $= 10^{-15}\,\mathrm{cm}^{-3}$) for a structural material, since mid-IR light can propagate through silicon with low loss due to small extinction coefficient, k, of silicon ($k = 10^{-9}$–10^{-4}).[26] For a coating material, we use aluminum, because it absorbs the wave leaked from the waveguide based on its large extinction coefficient ($k = 30$–100).[27] In addition, silicon and aluminum are relatively easy to integrate into cantilevers through microfabrication.

From an electromagnetic perspective, the silicon grating–waveguide on top of an aluminum layer is similar to a silicon grating totally surrounded by low index medium or air. The aluminum layer serves as a reflecting boundary or a mirror for the propagating waves in the silicon waveguide. Hence, the propagating modes in the silicon grating–waveguide on top of an aluminum coating are effectively equal to the propagating modes in an axisymmetric structure composed of twin silicon grating–waveguide structures. Therefore, the cantilever described in the previous paragraph possesses similar optical characteristics to HCG, which will be shown in the following paragraphs.

Our goal was to integrate gratings into the cantilever such that the resonance absorption of HCG occurs in mid-IR spectral region. There are several parameters that determine the resonance wavelengths of the grating such as grating period, Λ, grating duty cycle, η, grating depth, d_{gr}, the waveguide layer thickness, d_{wg}, the angle of incidence, θ, and the light polarization.[19–21,25] The photolithography resolution limits the ridges of the grating to be larger than 2–3 μm, therefore the grating period should be larger than 5 μm. For the simplicity, we set other geometric parameters as follows: $\eta = 0.5$, $d_{gr} = 0.5\,\mu$m, $d_{wg} = 1\,\mu$m. The waveguide layer thickness is related to the cantilever thermal conductance and mechanical compliance which are important factors for the cantilever thermomechanical sensitivity.[3]

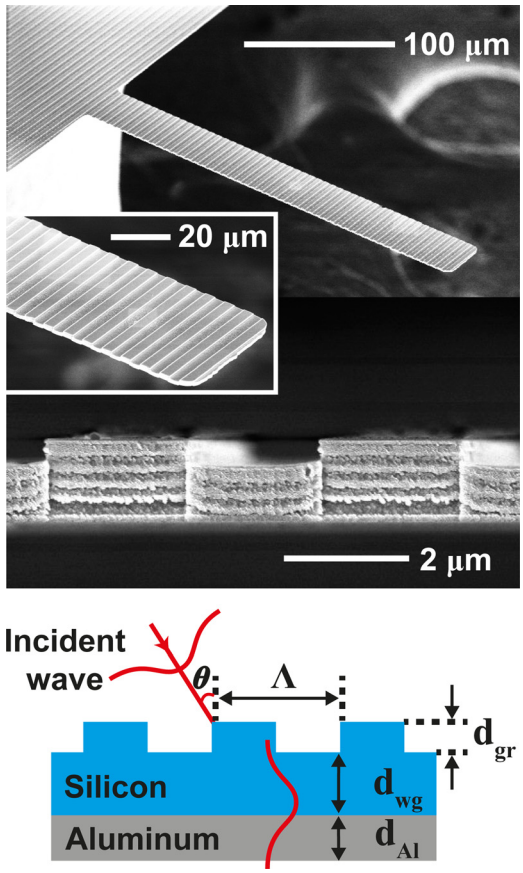

FIG. 1. Illustration and SEM micrographs of bimaterial cantilever based on silicon high contrast grating with aluminum coating on the bottom surface. A periodic 1D surface corrugation grating and a waveguide layer consist of single crystal silicon, while the bottom layer is aluminum. At a resonance wavelength of the grating, an incident wave couples to the waveguide layer and creates strong intensity distribution within the cantilever, resulting in strong cantilever absorptance. There are several parameters that determine the resonance wavelengths of the subwavelength grating: grating period, Λ, grating duty cycle, η, grating depth, d_{gr}, the waveguide layer thickness, d_{wg}, the angle of incidence, θ, and the light polarization.

We used a two-dimensional finite element model (COMSOL Multiphysics) to simulate the absorptance spectra of the cantilevers with different grating periods. Due to the symmetry of the geometry, we simulated a unit cell of the cantilever grating structure which corresponds to a single grating period. In the model, a plane electromagnetic wave is incident on the cantilever with either transverse electric (TE) or transverse magnetic (TM) polarization. The model calculates the cantilever absorptance from the ratio of the electromagnetic power loss within the cantilever to the incident light power. Since we will characterize the cantilever absorptance with randomly polarized light source in later section, we averaged the cantilever absorptance values calculated with TE and TM polarized light.

Figure 2(a) shows the calculated cantilever absorptance when the grating period is 5 μm with an angle of incidence of 0° or 30°. At the wavelength longer than the grating

[This article is copyrighted as indicated in the article. Reuse of AIP content is subject to the terms at: http://scitation.aip.org/termsconditions. Downloaded to] IP: 192.17.144.31 On: Fri, 10 Jan 2014 08:09:37

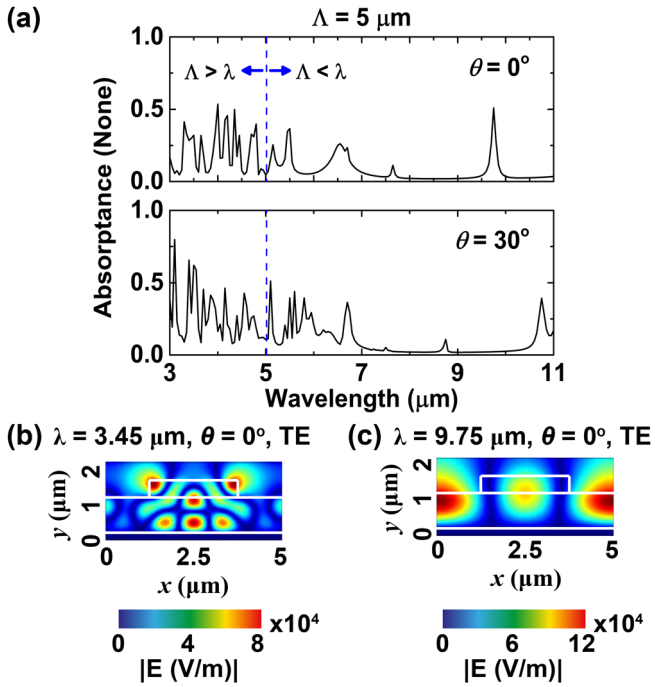

FIG. 2. Calculated IR absorptance and electric field amplitude distribution of a cantilever with HCG (grating period $\Lambda = 5\,\mu$m, duty cycle $\eta = 0.5$, grating depth $d_{gr} = 0.5\,\mu$m, waveguide thickness $d_{wg} = 1\,\mu$m) using a finite element model. (a) IR absorptance spectra when both TE and TM polarized wave are incident on the cantilever at either 0° or 30° angle. (b) and (c) Distribution of the electric field amplitude (|El) in a unit cell of the cantilever when a TE polarized wave is normally incident with a wavelength of either 3.45 or 9.75 μm.

period, an absorption peak due to a resonance mode in HCG appears at 9.75 μm for 0° angle of incidence and at 10.75 μm for 30° angle of incidence.[23,28] At the wavelength shorter than the grating period, multiple absorptance peaks appear, since higher-order modes of HCG occur.[23,28] Figures 2(b) and 2(c) show the distribution of the electric field amplitude, |El, in a unit cell of a cantilever when a plane wave with TE polarization incident at 0° angle of incidence. At the absorptance peak at 3.45 μm, multiple propagating modes in the waveguide interfere, and create a complex field distribution. At the absorptance peak at 9.75 μm, only a single propagating mode exists in the waveguide, and a simple standing wave pattern appears. In the same manner, we calculated the absorptance spectra of the cantilevers with grating periods of 5.5 μm. The simulation indicated that the grating period of 5.5 μm has resonance at the wavelengths 9.15–10.15 μm when the angle of incidence varies from 0° to 30°.

The aluminum layer thickness, d_{Al}, cantilever length, L, and cantilever width, w, are important for both the cantilever thermomechanical sensitivity and the compatibility with the optical cantilever deflection detection system.[3] There is an optimum value for the ratio of coating layer thickness to the structural layer thickness to maximize the thermal expansion mismatch stress.[19] The optimum ratio is typically larger than 0.2, thus the aluminum coating should be thicker than 200 nm for a 1 μm thick silicon cantilever. However, the evaporated aluminum film typically is under a compressive intrinsic stress[29] such that thick aluminum layer causes the cantilever to bend severely. When the cantilever bending is too large, the laser beam in the deflection readout reflects off the cantilever, deviates from the photodiode, and fails to read the cantilever deflection. For the cantilever to possess large thermomechanical sensitivity, the cantilever has to be long and narrow.[3] However, when the cantilever is too long, the intrinsic stress-induced cantilever deflection becomes too large. In addition, when the cantilever is too narrow, the optical cantilever deflection readout system cannot acquire sufficient signal. Based on these competing considerations, we selected the aluminum coating thickness as 100 nm, cantilever length as 460 μm, and cantilever width as 40 μm.

The HCG cantilevers are fabricated using a silicon-on-insulator (SOI) wafer with a 2.0 μm-thick device layer. We first pattern gratings using a conventional photolithography followed by an anisotropic etching of the silicon. The second photolithography patterns a mask for cantilevers, which is carefully aligned with the gratings. Deep reactive ion etching (DRIE) of the silicon using these patterns follows until the buried oxide is exposed. In order to release the cantilevers, windows around the cantilevers are patterned from the backside of the SOI wafer. We etch through the SOI handle layer from the backside using the buried oxide layer as an etch stop. Finally, we use a hydrofluoric acid (HF) solution to remove the oxide and release the cantilevers. Table I lists the dimensions of the fabricated cantilevers and a commercially obtained cantilever without HCG. The grating period has a length scale of the wavelength of interest. The commercially obtained cantilever also consists of a silicon and aluminum layers (Mikromasch, CSC17) and possesses relatively large IR sensitivity among commercial silicon based bimaterial cantilevers.[5]

III. CANTILEVER CHARACTERIZATION

Figure 3 shows the measured and calculated IR absorptance of the cantilevers. We obtained the cantilever IR absorptance using a Fourier transform infrared (FTIR) imaging spectrometer (Agilent, 680-IR spectrometer with 620-IR optical microscope). FTIR measured the reflectance and transmittance of the cantilever and subtracted them from unity to acquire the cantilever absorptance. The details of the FTIR measurement protocol are described elsewhere.[30] We also calculated cantilever IR absorptance using the finite element model when a plane wave with TE or TM polarization is incident on a cantilever at incidence angles of 10°–30° with a step size of 2°. The dashed lines in Fig. 3 correspond to the average values of the calculated cantilever absorptance for all the light polarizations and angles of incidence, which

TABLE I. Description of cantilevers.

Cantilever	A	B	C
Grating period Λ (μm)	5.07	5.45	…
Grating duty cycle η	0.51	0.46	…
Grating depth d_{gr} (μm)	0.43	0.48	…
Waveguide layer thickness d_{wg} (μm)	1.35	0.94	1.61
Aluminum thickness d_{Al} (nm)	100	100	16
Cantilever length L (μm)	463	465	441
Cantilever width w (μm)	42	41	40

[This article is copyrighted as indicated in the article. Reuse of AIP content is subject to the terms at: http://scitation.aip.org/termsconditions. Downloaded to] IP: 192.17.144.31 On: Fri, 10 Jan 2014 08:09:37

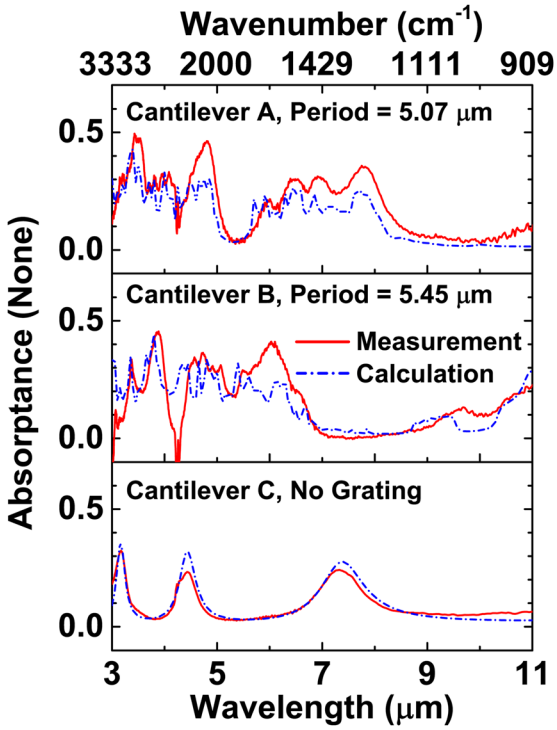

FIG. 3. Spectral absorptance of (a) cantilever A, (b) cantilever B, and (c) cantilever C for the 3–11 μm wavelength region, when randomly polarized waves are incident on a cantilever at a range of angles (10°–30°). The solid lines show cantilever absorptance measured in an FTIR spectrometer. The dashed lines show calculation results from the finite element model.

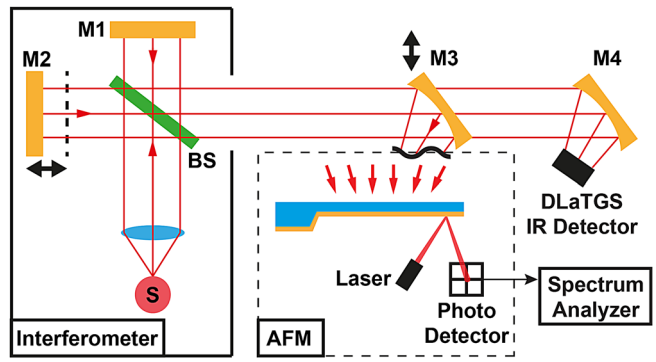

FIG. 4. Schematic of the experimental setup for measuring the cantilever IR responsivity and the IR spectrum of a thin film sample. The Michelson interferometer includes an IR emitter at 540 °C (S), fixed mirror (M1), a moving mirror (M2), and a beam splitter (BS). A concave mirror (M3) focuses the intensity modulated broadband IR light onto a bimaterial cantilever mounted in a commercial AFM. A spectrum analyzer performs fast Fourier transform on the cantilever deflection signal acquired by the AFM. When M3 is removed from the beam path, the light from interferometer is focused onto a DLaTGS IR detector via a concave mirror (M4).

compare well with the measured values. Here, the absorptance spectra of the cantilevers with HCG, cantilevers A and B, have several bands that are the superposition of multiple resonance absorption bands. The multiple absorption bands occur when HCG cantilevers are subject to either randomly polarized light or light from a range of incidence angles. Thus, the superposition of absorption bands occurring in cantilevers A and B is due to the optical configuration of the characterization system. The spectrometer uses a non-polarized light source (a globar). In addition, a Schwartzschild objective with a numerical aperture of 0.5 and central obscuration is used to illuminate light on a cantilever, resulting in light spread over various angles of incidence (10°–30°).[31,32]

The amplitudes and bandwidths of the absorption bands increase in the cantilevers with HCG over the mid-IR. The average absorption peak amplitudes of cantilevers A and B range 0.35–0.36, while the average peak amplitude of cantilever C is 0.26. More importantly, the total bandwidth (defined as the sum of the bandwidths of the absorption bands with amplitude >0.2) of cantilevers A and B ranges 2.8–4.1 μm, while the total bandwidth of cantilever D is 1 μm. Therefore, the cantilevers with HCG have about 3–4X larger total bandwidths as compared to the cantilever with a smooth surface.

Figure 4 shows an experimental setup that measures cantilever spectral responsivity. The setup consists of a commercial FTIR spectrometer system (Bruker, Vertex 70) and an AFM system (Agilent, PicoPlus).[17,18] The Michelson interferometer produces an intensity modulated signal from broadband light, where the modulation frequency is different for each wavelength. The modulation frequency, f, is related to the wavelength, λ, by the relation $f = 2v/\lambda$, where v is the velocity of the moving mirror in the interferometer. The intensity modulated beam was focused on a cantilever mounted in the AFM, resulting in a periodic cantilever bending. The optical readout in the AFM measured the cantilever tip displacement. A spectrum analyzer (Stanford Research Systems, SR780) performed fast Fourier transform on the optical readout signal and recorded cantilever tip displacement as a function of the wavelength. The optical flux at the cantilever position normalized the cantilever tip displacement to obtain the responsivity. A deuterated L-alanin-doped triglycine sulfate (DLaTGS) IR detector in the FTIR spectrometer could also measure the interferometer output and was used for IR spectroscopy experiment which is described in the following section.

In addition, we calculated cantilever responsivity employing a model relating incident radiation, heat transfer, temperature distribution in the cantilever, and thermal expansion mismatch bending.[30] This model used the cantilever absorptance values obtained from the finite element model. The finite element model calculated the average values of the cantilever absorptance for TE and TM polarizations and the angles of incidence of 0°–15°, since the responsivity measurement setup had a non-polarized light source and used a spherical mirror to focus the light onto a cantilever. To account for the heat transfer from the cantilever to air, the responsivity model used an effective thermal conductance to air, G_a, = 30 μW/K for cantilevers A, B, and C, and $G_a = 20$ μW/K for cantilever D. These values of G_a provide model fit and are close to G_a for a silicon nitride-gold cantilever with similar dimensions.[33]

Figure 5 shows the measured and calculated IR responsivity of the cantilevers in the mid-IR. On average, the cantilevers with HCG have 13–47X greater responsivity than the cantilever without HCG, cantilever C. Average value of the responsivity is 316 pm/μW for cantilever A, 1181 pm/μW for

[This article is copyrighted as indicated in the article. Reuse of AIP content is subject to the terms at: http://scitation.aip.org/termsconditions. Downloaded to] IP: 192.17.144.31 On: Fri, 10 Jan 2014 08:09:37

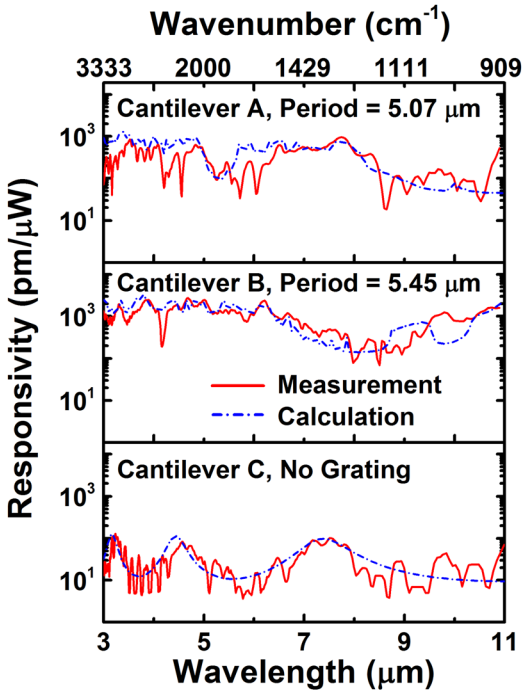

FIG. 5. Measured and predicted cantilever responsivity over the 3–11 μm wavelength region when randomly polarized waves are incident on a cantilever at a range of angles 0°–15°.

cantilever B, and 25 pm/μW for cantilever C. Using an average InvOLS value of the cantilevers (248 nm/V), the responsivity values of the HCG cantilevers in the unit of V/W can be known which range 1.2–4.7 kV/W. Other than enhanced cantilever absorptance, the improvement in the ratio of coating layer thickness to the structural layer thickness, d_{Al}/d_{wg}, is also responsible for the improved responsivity of the HCG cantilevers.[19] d_{Al}/d_{wg} is 0.07–0.1 for the HCG cantilevers, while d_{Al}/d_{wg} is 0.01 for cantilever C. Since d_{Al}/d_{wg} value of the HCG cantilevers is close to the optimum value (~0.2) as compared to cantilever C, HCG cantilevers are subject to larger thermal expansion mismatch stress when the same amount of heating power is applied.

We characterized the noise equivalent power, *NEP*, and detectivity, *D**, of the cantilevers.[3,6,19] Table II lists the measured *NEP*, *D** based on the average value of the cantilever responsivity. Thermomechanical noise of the cantilever and the noise from optical readout limit our IR power measurement.[9] The cantilever responsivity measurement setup recorded the noise floor while there is no IR heating on a cantilever. The noise floor equivalent tip displacement of the HCG cantilevers was on the order of 1 pm when a measurement bandwidth was 78 mHz. We normalized the noise equivalent cantilever tip displacement by both its responsivity and square root of the measurement bandwidth to obtain *NEP* which was on the order of 1 nW Hz$^{-1/2}$. Another important figure of merit for photodetectors is specific detectivity which is defined as $D^* = A^{1/2}/NEP$, where A is the area of the photosensitive region of the detector. Based on the cantilever surface areas and their *NEP*, *D** of the HCG cantilevers range 10^6–10^7 cm Hz$^{1/2}$ W^{-1}. For comparison, bolometer type IR detectors have *D** on the order of 10^8 cm Hz$^{1/2}$ W^{-1} and liquid-nitrogen-cooled mercury-cadmium-telluride (MCT) detectors have *D** on the order of 10^{10} cm Hz$^{1/2}$ W^{-1}.[14] Clearly, there is room for improving microcantilevers; however, this is the first example where cantilevers are approaching the capabilities of established monolithic detector technologies.

TABLE II. Microcantilever performance figures of merit.

Cantilever	A	B	C
Responsivity R (pm μW^{-1})	316	1181	25
Noise equivalent power *NEP* (nW Hz$^{-1/2}$)	6.7	0.5	47.2
Detectivity D* (cm Hz$^{1/2}$ W^{-1})	2.9×10^6	2.6×10^7	2.8×10^5

IV. AN APPLICATION TO INFRARED SPECTROSCOPY

The large IR responsivity of the HCG cantilever enables the cantilever based transmission IR spectroscopy with a Michelson interferometer, as shown in Fig. 4. To demonstrate the transmission IR spectroscopy, we obtained absorbance spectra of thin polyimide (PI) films. Absorbance, in IR spectroscopy, indicates a logarithmic ratio of incident IR power to transmitted IR power. The PI films are free-standing membranes with the thicknesses of 2.4, 3.6, and 8.3 μm supported by metallic frames at the edges. To prepare the PI films, we spin coated PI solution (HD Microsystems, PI-2555) on glass substrates and cured them at 300 °C for 1 h. Then, to transfer the PI films on the metallic frames, we bonded the metallic frames on top of the PI films with an adhesive, soaked them in hot water (90 °C) for 12 h, and detached the metallic frames from the glass substrates. A profilometer measured the thickness of the PI films which were remained on the glass substrates. A PI membrane was positioned in the beam path between the interferometer exit and a cantilever shown in Fig. 4. With a sample, we measured the cantilever deflection, z_t, arising from the transmitted beam intensity. Then, we removed the sample and measured the cantilever deflection, z_0, as a reference. Theoretically, the cantilever deflection has a linear relation to the incident radiative power, thus the sample absorbance can be calculated by $A = -\log_{10}(z_t/z_0)$. When we measured the absorbance spectrum with a DLaTGS IR detector in the FTIR system, we removed a spherical mirror (M3) in Fig. 4 which directed the interferometer output to the cantilever.

Figure 6(a) shows the absorbance spectra of PI films measured by cantilever B and the DLaTGS detector (spectral resolution = 16 cm^{-1}) in the wavelength range 3.3–7 μm. The spectra measured by both detectors resolve the absorbance bands at 5.8 and 6.6 μm and compare well. Cantilever B provides signal to noise ratio of 2–10 at 3.3–7 μm with 8.3 μm thick PI sample when the signal is averaged over 20 scan. However, cantilever C has low signal to noise ratio (~1) with the same sample such that absorbance spectrum is unobtainable. For this comparison, we averaged the DLaTGS detector over 20 scans as well. Importantly, the results show that the cantilever response to the incident power is linear such that the absorbance value linearly increases with the increasing sample thickness. Figure 6(b) shows the absorbance value at 5.8 and 6.6 μm as a function

[This article is copyrighted as indicated in the article. Reuse of AIP content is subject to the terms at: http://scitation.aip.org/termsconditions. Downloaded to] IP: 192.17.144.31 On: Fri, 10 Jan 2014 08:09:37

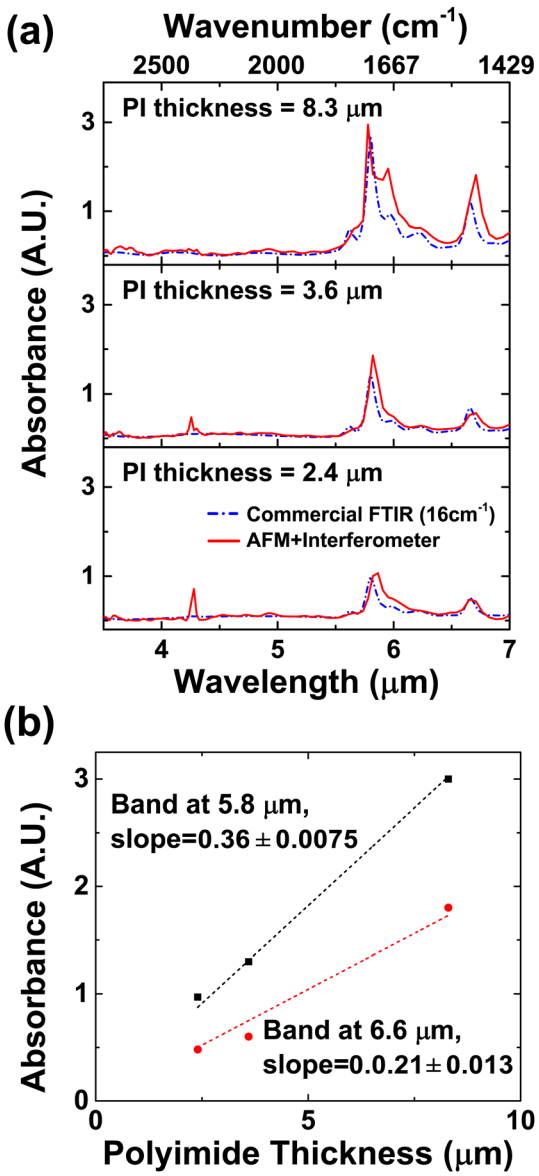

FIG. 6. Measured IR absorbance spectra of PI films at the wavelength region between 3.3 and 7 μm. (a) IR absorbance spectra of 2.4, 3.6, and 8.3 μm thick PI films obtained by cantilever B (solid line) and a DLaTGS IR detector (dash line). (b) Absorbance value measured by cantilever B near 5.8 (square) and 6.6 μm (circle) as a function of the PI film thickness.

of the PI film thickness, which verifies the linear relation between absorbance value measured by the cantilever and the sample thickness.

The HCG bimaterial cantilever has performance comparable to a DLaTGS detector which is prevalent in low-end commercial FTIR systems. The signal to noise of the HCG cantilever and a commercial DLaTGS detector are comparable; the DLaTGS detectors have an order of magnitude smaller responsivity ($\sim$100 V/W) and an order of magnitude larger D^* ($\sim 10^8$ cm Hz$^{1/2}$ W^{-1}) than the HCG cantilever. Furthermore, the HCG cantilever response is a linear function to the incident IR power similar to the DLaTGS detector. Some IR detectors such as mercury-cadmium-telluride (MCT) detector have nonlinear response to the incident radiation, which requires additional data correction process for the quantitative study based on IR spectroscopy. The response speed of the HCG cantilever, however, is limited by its thermal time constant which is on the order of $\sim$1 ms. This response speed is still compatible with a commercial Michaelson interferometer.

V. CONCLUSION

We designed and fabricated bimaterial cantilevers based on a silicon HCG. The cantilevers with HCG had about 3–4X larger total IR absorptance bandwidths and 30% improvement in absorptance peak amplitude as compared to the cantilever without HCG. The strong IR absorption by HCG cantilevers is due to the resonance modes in HCG, which is confirmed by good agreement between measured cantilever performance and finite element simulations. Based on the improved IR absorptance, the HCG cantilevers had 13–47X greater responsivity values than the cantilever without HCG. The HCG cantilevers had *NEP* as small as 0.6 nW Hz$^{-1/2}$ and detectivity, D^*, as small as 2.2×10^7 cm Hz$^{1/2}$ W^{-1}. The improved responsivity of the HCG cantilevers enabled transmission IR spectroscopy with a Michelson interferometer. Overall, the HCG cantilevers have signal to noise characteristics that are comparable to a low-end commercial FTIR system. The HCG cantilever obtained IR absorbance spectra of polyimide films and exhibited linear response to the incident IR light. The IR absorptance amplitude, total bandwidth, and the active wavelengths for the HCG cantilever are dependent on the geometric parameters for HCG, hence there is the potential for additional optimization.

ACKNOWLEDGMENTS

We gratefully acknowledge AFOSR FA9550-12-1-0089 and National Science Foundation Grant No. CHE 0957849. We also acknowledge the Congressionally Directed Medical Research Program Postdoctoral Fellowship BC101112 to Matthew V. Schulmerich.

[1]P. G. Datskos, N. V. Lavrik, S. R. Hunter, S. Rajic, and D. Grbovic, Opt. Lett. **37**, 3966 (2012).
[2]J. R. Barnes, R. J. Stephenson, C. N. Woodburn, S. J. Oshea, M. E. Welland, T. Rayment, J. K. Gimzewski, and C. Gerber, Rev. Sci. Instrum. **65**, 3793 (1994).
[3]B. Kwon, M. Rosenberger, R. Bhargava, D. G. Cahill, and W. P. King, Rev. Sci. Instrum. **83**, 015003 (2012).
[4]B. Kwon, M. V. Schulmerich, L. J. Elgass, R. Kong, S. E. Holton, R. Bhargava, and W. P. King, Ultramicroscopy **116**, 56 (2012).
[5]B. Kwon, C. Wang, K. Park, R. Bhargava, and W. P. King, Nanoscale Microscale Thermophys. Eng. **15**, 16 (2011).
[6]J. Varesi, J. Lai, T. Perazzo, Z. Shi, and A. Majumdar, Appl. Phys. Lett. **71**, 306 (1997).
[7]Y. Zhao, M. Mao, R. Horowitz, A. Majumdar, J. Varesi, P. Norton, and J. Kitching, J. Microelectromech. Syst. **11**, 136 (2002).
[8]C. W. Van Neste, L. R. Senesac, D. Yi, and T. Thundat, Appl. Phys. Lett. **92**, 134102 (2008).
[9]P. G. Datskos, N. V. Lavrik, and S. Rajic, Rev. Sci. Instrum. **75**, 1134 (2004).
[10]M. R. Rosenberger, B. Kwon, D. G. Cahill, and W. P. King, Sens. Actuators, A **185**, 17 (2012).
[11]C. Canetta and A. Narayanaswamy, Appl. Phys. Lett. **102**, 103112 (2013).
[12]A. Rogalski, *Infrared Detectors*, 2nd ed. (Taylor & Francis, New York, NY, 2010).
[13]F. Niklaus, C. Vieider, and H. Jakobsen, Proc. SPIE **6836**, 68360D (2007).
[14]A. Rogalski, *Infrared Detectors*, 2nd ed. (CSC Press, New York, 2011).

[This article is copyrighted as indicated in the article. Reuse of AIP content is subject to the terms at: http://scitation.aip.org/termsconditions. Downloaded to] IP: 192.17.144.31 On: Fri, 10 Jan 2014 08:09:37

[15]D. Grbovic, N. V. Lavrik, P. G. Datskos, D. Forrai, E. Nelson, J. Devitt, and B. McIntyre, Appl. Phys. Lett. **89**, 073118 (2006).
[16]R. Bhargava, Appl. Spectrosc. **66**, 1091 (2012).
[17]W.-C. Hsu, J. K. Tong, B. Liao, B. R. Burg, and G. Chen, Appl. Phys. Lett. **102**, 051901 (2013).
[18]L. Tetard, A. Passian, R. H. Farahi, B. H. Davison, and T. Thundat, Opt. Lett. **36**, 3251 (2011).
[19]J. Lai, T. Perazzo, Z. Shi, and A. Majumdar, Sens. Actuators, A **58**, 113 (1997).
[20]S. Sadat, Y. J. Chua, W. Lee, Y. Ganjeh, K. Kurabayashi, E. Meyhofer, and P. Reddy, Appl. Phys. Lett. **99**, 043106 (2011).
[21]M. Klanjšek Gunde and M. Maček, Phys. Status Solidi A **183**, 439 (2001).
[22]Y. Zhou, M. C. Y. Huang, C. Chase, V. Karagodsky, M. Moewe, B. Pesala, F. G. Sedgwick, and C. J. Chang-Hasnain, IEEE J. Sel. Top. Quantum Electron. **15**, 1485 (2009).
[23]C. J. Chang-Hasnain, Semicond. Sci. Technol. **26**, 014043 (2011).
[24]V. Karagodsky and C. J. Chang-Hasnain, Opt. Express **20**, 10888 (2012).
[25]S.-F. Lin, C.-M. Wang, T.-J. Ding, Y.-L. Tsai, T.-H. Yang, W.-Y. Chen, and J.-Y. Chang, Opt. Express **20**, 14584 (2012).
[26]*Handbook of Optical Constants of Solids*, edited by E. D. Palik (Academic, New York, 1985), Vol. III.
[27]Q. M. Brewster, *Thermal Radiative Transfer and Properties* (John Wiley & Sons, Inc, New York, 1992).
[28]J.-N. Liu, M. V. Schulmerich, R. Bhargava, and B. T. Cunningham, Opt. Express **19**, 24182 (2011).
[29]R. Abermann, Vacuum **41**, 1279 (1990).
[30]B. Kwon, J. Jiang, M. V. Schulmerich, Z. Xu, R. Bhargava, G. L. Liu, and W. P. King, Sens. Actuators, A **199**, 143 (2013).
[31]B. J. Davis, P. S. Carney, and R. Bhargava, Anal. Chem. **82**, 3487 (2010).
[32]B. J. Davis, P. S. Carney, and R. Bhargava, Anal. Chem. **82**, 3474 (2010).
[33]A. Narayanaswamy and N. Gu, ASME Trans. J. Heat Transfer **133**, 042401 (2011).

[This article is copyrighted as indicated in the article. Reuse of AIP content is subject to the terms at: http://scitation.aip.org/termsconditions. Downloaded to] IP: 192.17.144.31 On: Fri, 10 Jan 2014 08:09:37